Poultry Science

Effects of freezing on the gelation behaviors of liquid egg yolks affected by saccharides: thermal behaviors and rheological and structural changes

Zihong Ma ,* Mingmin Qing,* Jingnan Zang,* Yonghao Xu,* Xin Gao,* Yuan Chi,† and Yujie Chi *,[1]

*College of Food Science, Northeast Agricultural University, Harbin 150030, P. R. China; and †College of Engineering, Northeast Agricultural University, Harbin 150030, P. R. China

ABSTRACT Monitoring and controlling the freezing process and thermal properties of foods is an important means to understand and maintain product quality. Saccharides were used in this study to regulate the gelation of liquid egg yolks induced by freeze–thawing; the selected saccharides included sucrose, L-arabinose, xylitol, trehalose, D-cellobiose, and xylooligosaccharides. The regulatory effects of saccharides on frozen egg yolks were investigated by characterizing their thermal and rheological properties and structural changes. The results showed that L-arabinose and xylitol were effective gelation regulators. After freeze–thawing, the sugared egg yolks exhibited a lower consistency index and fewer rheological units than those without saccharides, indicating controlled gelation. Weaker aggregation of egg yolk proteins was confirmed by smaller aggregates observed by confocal laser scanning microscopy and smaller particle sizes. Saccharides alleviated the freeze-induced conversion of α-helices to β-sheets in egg yolk proteins, exposing fewer Trp residues. Overall, L-arabinose showed the greatest improvement in regulating the gelation of egg yolks, followed by xylitol, which is correlated with its low molecular weight.

Key words: frozen egg yolk processing, food freezing, cryopreservation, thermal behavior

2024 Poultry Science 103:103657
https://doi.org/10.1016/j.psj.2024.103657

INTRODUCTION

Egg yolk contains approximately 50 wt% water, 30 wt% lipids, 16 wt% proteins, and some other substances in minor quantities (Ma et al., 2023). It can be regarded as an extremely complex natural supramolecular assembly of lipids and proteins (Zhao et al., 2024). Egg yolk is composed of insoluble protein aggregates (granules, primarily high-density lipoproteins (**HDL**) and phosvitins) suspended in a transparent yellow matrix (plasma) that contains soluble livetins and low-density lipoproteins (**LDL**) (Anton, 2013; Liu et al., 2023a). Egg yolks are increasingly employed in the food industry due to their remarkable nutritional, organoleptic, and functional properties (Chi and Ma, 2023; Liu, et al., 2023b; Liu, et al., 2024). Recently, the development and application of liquid egg yolk products have gained more popularity than shell eggs in terms of standardized processing and easier handling and transportation (Chi and Ma, 2023; Liu et al., 2024; Zhao et al., 2024). However, extending the shelf-life of liquid egg yolks is still challenging because they are highly perishable, and the major proteins in egg yolks (LDL) are susceptible to external processing conditions such as thermal pasteurization; only mild pasteurization is applied, thus limiting the possibilities for bacterial decontamination (Zhao et al., 2023a; Zhao et al., 2023b).

The long transportation radius of China is one of the key issues hindering the flexible circulation of primary agricultural products. The development of cold chain techniques has brought enormous benefits to human beings in terms of prolonging shelf-life and maintaining food freshness (Ma et al., 2023). Freezing, one of the most frequently used cold chain techniques, has been utilized in the food industry for more than a century (Tian et al., 2020). However, the water/ice transition during freezing inevitably leads to dehydration and disruption of food components, thus causing quality degradation of food products (Lu et al., 2023; Lu et al., 2024). Maintaining and improving the quality of frozen foods is conducive to the sustainable development of the frozen food industry.

In some cases, liquid egg yolks are commercially frozen (−18°C) to extend their shelf-life (up to a year), and frozen egg products with a longer sale radius can be put on the market (even overseas) pertinently during periods of low egg production to compensate for the shortage of fresh shell eggs. However, quality degradation of frozen egg yolks has also been reported, as manifested by a loss

Received January 30, 2024.
Accepted March 11, 2024.

[1]Corresponding author: yjchi323@126.com

in fluidity and a gel-like texture after freeze−thawing (Ma et al., 2021; Ma et al., 2023). This phenomenon has been termed frozen egg yolk gelation. The gelation of frozen-thawed egg yolks is not conducive to the development of the egg processing industry. Numerous researchers have attributed this undesirable phenomenon to the denaturation and aggregation of lipoproteins (mainly LDLs) caused by ice crystallization (Primacella et al., 2018; Wang et al., 2020; Wang et al., 2021a).

Investigating the factors that control ice crystallization and growth in food materials during freezing is interesting and meaningful. Monitoring and controlling the freezing process and thermal properties of foods is an important means of understanding and maintaining product quality. The thermal properties of frozen foods, including the initial freezing point (T_{if}), crystallization temperature (T_c), onset of ice melting (T_m'), apparent specific heat capacity (C_{app}), etc., are required to regulate the freezing processes, and provide the ideal frozen storage and transportation conditions (Kumar et al., 2018). Cryoprotectants have been widely used in food freezing to regulate the freezing process of foods. Although there are already some reports on the use of sugars or other biomolecular additives to improve the gelation deterioration of frozen egg yolks, to the best of our knowledge, none of these publications have focused on the thermal properties/freezing behaviors of yolk freezing (Fei et al., 2021; Li et al., 2023; Xu et al., 2024). Our previous study has confirmed that saccharides could alter the water behaviors of egg yolks (Ma et al., 2023), but the thermal properties/freezing behaviors of yolk freezing are still unclear. Therefore, this study mainly investigated how saccharides regulate the gelation behaviors of frozen egg yolks by monitoring their thermal properties. Saccharides, including L-arabinose, xylitol, trehalose, D-cellobiose, and xylooligosaccharides, were selected from previous studies due to their cryoprotective abilities in other food systems or their low-calorie properties (Zhang et al., 2019; Ankita and Nain, 2020; Su et al., 2020; Scettri and Schievano, 2022; Tan et al., 2022), and sucrose was used as a control. To evaluate the regulatory effect of these saccharides, the rheological and structural properties of the egg yolks were also monitored to characterize the gelation degree. Overall, our findings can be used to regulate the gelation behaviors of frozen egg yolks, develop new frozen egg yolk formulas, and optimize processing conditions.

MATERIALS AND METHODS

Materials

Fresh hen eggs (approximately 70−80 eggs in each batch) were purchased from a local market and preserved at 4 ± 2°C for a maximum of 7 d. L-arabinose (molecular weight (**Mw**): 150.13) and trehalose (Mw: 342.297) were obtained from Jiangsu Caiwei Biotechnology Co., Ltd. (Xuzhou, China). Sucrose (Mw: 342.297) was obtained from Guangzhou Fuzheng Donghai Food Co., Ltd. (Guangzhou, China). Xylitol (Mw: 152.146), D-cellobiose (Mw: 342.29), xylooligosaccharides (average Mw: 300.28−1050.9), and Nile red were obtained from Shanghai Yuanye Bio-Technology Co., Ltd. (Shanghai, China). Sodium chloride (**NaCl**) was obtained from Tianjin Kaitong Chemical Reagent Co., Ltd. (Tianjin, China). Urea was obtained from Tianjin Aopusheng Chemical Co., Ltd (Tianjin, China). Sodium dodecyl sulfate (**SDS**) and bicinchoninic acid (**BCA**) protein assay kits were obtained from Beijing Solarbio Science & Technology Co., Ltd. (Beijing, China). Nile blue was obtained from Shanghai Macklin Biochemical Technology Co., Ltd. (Shanghai, China).

Preparation of Egg Yolk Samples

Liquid egg yolks were collected by breaking shell eggs (approximately 750−800 mL in each batch) manually and the collected egg yolks (without yolk membranes) were then carefully stirred until homogenization (ES35A-Pro, LabTech, Inc., Beijing, China). The saccharides (5 wt%) were then mixed with homogenized egg yolks and slowly stirred until they were fully dissolved. The bubbles in the egg yolks (if any) were removed by mild sonication (KQ-800DE, Kunshan Ultrasonic Instruments Co., Ltd., Kunshan, China). Egg yolk samples mixed with saccharides were labeled as $\mathbf{EY_{sucrose}}$, $\mathbf{EY_{arabinose}}$, $\mathbf{EY_{xylitol}}$, $\mathbf{EY_{trehalose}}$, $\mathbf{EY_{cellobiose}}$, and $\mathbf{EY_{xylooligosaccharides}}$. Egg yolks without additives were denoted as **FEY**.

Freezing and Thawing of Egg Yolk Samples

The prepared egg yolk samples (30 g) were transferred to 50-mL centrifuge tubes and placed in a freezer (BCD−258WTPZM, Hefei Midea Refrigerator Co., Ltd., Hefei, China) at −18°C for 3 d, after which they were subsequently thawed at ambient temperature for 12 h before analysis.

Characterization of the Thermal Properties of Unfrozen Egg Yolk Samples

Monitoring the Freezing Process by Freezing Curve Method. Measurements were conducted using a temperature recorder (T20BL-EX, Shenzhen Huahanwei Technology Co., Ltd., Shenzhen, China). The prepared egg yolks (unfrozen, 30 g) were transferred to 50-mL centrifuge tubes, and the subsidiary temperature sensor was inserted and fixed in the center of the samples. The samples were then stored in the same freezer above at −18°C with the temperature recorded every 60 s. The T_{if} and the time required to pass through the maximum ice crystal formation zone (t_z) were obtained.

Monitoring the Freezing Process by Differential Scanning Calorimetry (DSC) Method. A differential scanning calorimeter (DSC250, TA Instrument-Waters Ltd., DE) was used to monitor the DSC thermograms of egg yolk samples. Before measurements, the DSC was calibrated for temperature and heat flow using indium (melting

temperature ($\boldsymbol{T_m}$) = 156.6°C, enthalpy of melting ($\boldsymbol{\Delta H_m}$) = 28.60 J/g). Briefly, the prepared egg yolk samples (unfrozen, 5−10 mg) were transferred to aluminum pans and then hermetically sealed. An empty pan was used as a reference. The experiments were carried out in a nitrogen medium with a flow rate of 50 mL/min. The samples were first equilibrated at 25°C for 2 min, followed by a cooling program to −40°C at 10°C/min. After being held at −40°C for 2 min, the samples were then heated to 25°C at 10°C/min. The T_c, enthalpy of crystallization ($\boldsymbol{\Delta H_c}$), T_m', T_m, T_{if}, and ΔH_m were analyzed using built-in software (TRIOS, TA Instruments).

Determination of C_{app}. The C_{app} of unfrozen egg yolk samples was determined using the same DSC above based on the method described by Ding, et al. (2015). The experiments were carried out in a nitrogen medium with a flow rate of 50 mL/min. The samples were first equilibrated at 20°C for 2 min, followed by a cooling program to −80°C at 5°C/min. After being held at −80°C for 10 min, the samples were then heated to 20°C at 2°C/min. The freeze−thaw procedure was carried out on a blank pan, a standard material (sapphire), and egg yolk samples, respectively. The C_{app} of egg yolks was calculated using the equation below:

$$C_{app} = \frac{m_{std}}{m_{EY}} \times \frac{DSC_{EY} - DSC_b}{DSC_{std} - DSC_b} \times C_{p-std} \quad (1)$$

where m_{std} is the weight of the sapphire, mg; m_{EY} is the weight of the egg yolk sample, mg; DSC_{EY} is the heat flow of the egg yolk sample, mW; DSC_b is the heat flow of the blank pan, mW; DSC_{std} is the heat flow of the sapphire, mW; and $C_{p\text{-}std}$ is the specific heat capacity ($\boldsymbol{C_p}$) of standard sapphire, J/(g·°C).

Characterization of the Rheological Properties of Egg Yolk Samples

The rheological properties of the egg yolk samples were measured by a Modular Rotating Rheometer (HAAKE MARS60, Thermo Fisher Scientific (China) Co., Ltd., Shanghai, China).

Flow Behavior. The prepared egg yolks (unfrozen and frozen-thawed) were tiled on a parallel plate geometry (diameter, 35 mm). The parameters were set as follows: temperature, 20°C; gap distance, 0.3 mm; equilibrium time, 180 s; and shear rate, 0.1 to 100 1/s. The apparent viscosity and shear rate were fitted with the following power-law equation (Ma et al., 2021):

$$\eta = K \cdot \dot{\gamma}^{n-1} \quad (2)$$

where η is the apparent viscosity (Pa·s); K is the consistency index (Pa·s^n); $\dot{\gamma}$ is the shear rate (1/s); and n is the flow index.

Viscoelasticity. The prepared egg yolks (unfrozen and frozen-thawed) were tiled on a parallel plate geometry (diameter, 35 mm). The parameters were set as follows: temperature, 20°C; gap distance, 0.3 mm; equilibrium time, 180 s; frequency: 0.1 to 10 Hz. An oscillatory dynamic sweep was performed at a constant strain of 0.1% (within the linear viscoelastic region). The storage modulus (G') and loss modulus (G'') were recorded. The complex modulus (G^*) and the loss tangent ($tan\ \delta$) were calculated by using the following equations:

$$G^* = \sqrt{(G')^2 + (G'')^2} \quad (3)$$

$$tan\ \delta = G''/G' \quad (4)$$

In addition, the obtained G^* was fitted with the following power-law equation (Gabriele, et al., 2001):

$$G^* = A_F \cdot \omega^{1/z} \quad (5)$$

where G^* is the complex modulus in Pa; ω is the frequency in Hz; z is the number of rheological units correlated with one another in the 3D structure; and A_F (Pa·s$^{1/z}$) is the strength of the interactions between those units.

Characterization of the Structural Properties of Egg Yolk Samples

Molecular Interactions Maintaining the Egg Yolk Matrix. The molecular interactions maintaining the egg yolk samples were determined using the method described by Wang et al. (2021b). In total, 1 g of the prepared egg yolk samples (unfrozen and frozen-thawed) was dissolved in 3 denaturants (30 mL): 1 wt% NaCl solution (**S1**), 1 mol/L urea solution (**S2**), and 1 wt% SDS solution (**S3**). The mixtures were vortexed (LP, Thermo Fisher Scientific (China) Co., Ltd., Shanghai, China) until the samples were completely dispersed. Subsequently, the mixtures were centrifuged (5810R, Eppendorf AG, Hamburg, Germany) at 8,000 × g (4°C, 15 min), and the protein content in the supernatant was measured using a BCA protein assay kit with a microplate reader (SpectraMax reg iD3, Molecular Devices (Shanghai) Co., Ltd., Shanghai, China). The rate of change in protein concentration after treatment with different denaturants was quantified according to the following equation:

$$\text{Change rate } (\%) = \left(C_1 - C_0\right)/C_0 \times 100\% \quad (6)$$

where C_0 and C_1 represent the protein concentrations in distilled water and various denaturants, respectively. All measurements were performed at least thrice.

Macro- and Micro-observations. The macroscopic appearance of frozen-thawed egg yolk samples was observed by recording their fluidity. Briefly, unfrozen egg yolk samples were transferred to glass vials and frozen in the same freezer at −18°C for 3 d before thawing (the vials were inverted) at ambient temperature for 4 h. The fluidity of the samples was recorded and compared. FEY without freeze−thawing was also used for comparison.

The microappearance of frozen-thawed egg yolk samples was observed by confocal laser scanning microscopy (**CLSM**) (TCS SP8, Leica Microsystems, Wetzlar, Germany) by consulting Wang et al. (2021a). Egg yolk

samples (1 g) were dispersed in 15 mL of distilled water and vortexed for 15 min. When the mixture was being vortexed, Nile blue (15 μL, 1 mg/mL in propyl alcohol) and Nile red (15 μL, same concentration in the same buffer above) were added and mixed in the dark. The stained egg yolk samples (10 μL) were pipetted onto a microscope slide and covered with special cover glass. The surrounding of the cover glass was then sealed with film-forming liquids (the main active ingredient: nitrocellulose) to avoid any leakage of the samples. The prepared microscope slides were then observed by the CLSM using an objective lens (40 ×). FEY without freeze–thawing was also used for comparison. Nile red was excited at 488 nm, and the emission wavelength was between 500 and 540 nm. Nile blue was excited at 640 nm, and the emission wavelength was between 650−700 nm.

Particle size. The particle size of frozen-thawed egg yolk samples was measured using the method described in our previous studies (Ma et al., 2021; Zang et al., 2023). Frozen-thawed egg yolk samples were dispersed in distilled water at a sample concentration of 0.2% (w/v). The dispersions were then magnetically stirred until homogenization. The diluted samples were subjected to particle size measurements using a particle size and shape analyzer (Sync, Microtrac Inc., FL). FEY without freeze–thawing was also used for comparison.

*Fourier Transform Infrared Spectrum (**FTIR**).* The prepared egg yolk samples (unfrozen and frozen-thawed) were lyophilized (pilot10-15EP, BoYiKang (Beijing) Instrument Co., Ltd., Beijing, China) and scanned using an FTIR Spectrometer (Nicolet iS 50, Thermo Fisher Scientific (China) Co., Ltd., Shanghai, China) equipped with an attenuated total reflection (**ATR**) scanning attachment to record FTIR spectra. The scans were conducted between 4,000 and 400/cm. The raw FTIR spectra were processed using OMNIC software (9.2, Thermo Fisher Scientific Inc., MA). The second derivatives of the amide I spectra (1,700/cm−1,600/cm) were obtained using Origin software (OriginPro 2021, OriginLab Co., MA).

Intrinsic Fluorescence Spectrum. The intrinsic fluorescence spectrum of egg yolk samples was measured by consulting Wang et al. (2021a). The prepared egg yolk samples (unfrozen and frozen-thawed) were dissolved in 0.01 mol/L PBS buffer (pH 7.2−7.4). The diluted samples (protein concentration: 1 mg/mL) were scanned with a fluorescence spectrophotometer (F-7,100, Hitachi Hi-Tech Co., Ltd., Kyoto, Japan) 3 times. Before testing, the spectrophotometer was zeroed using the PBS buffer mentioned above. The parameters were set as follows: excitation wavelength, 280 nm; emission wavelength, 300 to 420 nm; scan speed, 60 nm/min; emission and excitation slit width, 5 nm; and response, 8.0 s.

Statistical Analysis

At least 3 replicates were used for each measurement, and all the results are presented as the means ± standard deviations (**SDs**). SPSS software (26.0, SPSS Inc., Chicago, IL) was used to perform the statistical analysis, including analysis of variance (**ANOVA**) and Student's t test, with a significant difference of $P < 0.05$. OriginPro 2021 was used to plot the figures.

RESULTS AND DISCUSSION

Thermal Properties of Egg Yolk Samples

Freezing Curve. The freezing curves of the egg yolk samples were obtained by real-time temperature monitoring. Figure 1A displays the typical freezing curve of a food system (FEY as an example). We can see that the

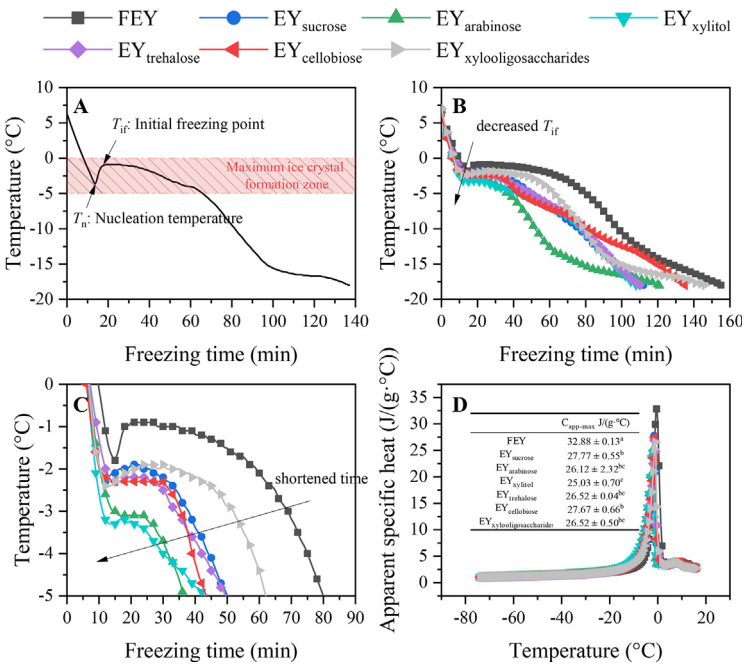

Figure 1. Changes in the freezing curves and C_{app} of egg yolks. Note: typical freezing curve of FEY (A), freezing curves of sugared egg yolk (B), maximum ice crystal formation zone (C), and C_{app} (D).

Table 1. Thermal parameters of egg yolk samples obtained by freezing curve and DSC thermogram.

	Freezing curve		DSC thermogram					
	T_{if} /°C	t_z / min	T_c /°C	ΔH_c / J/g	T_m' /°C	T_m /°C	ΔH_m	T_{if} /°C
FEY	-0.97 ± 0.06^{a}	69.33 ± 5.03^{a}	-16.82 ± 0.95^{a}	114.41 ± 3.97^{a}	-8.63 ± 0.51^{a}	-0.33 ± 0.31^{a}	108.28 ± 3.47^{a}	-1.02 ± 0.10^{a}
$EY_{sucrose}$	-2.05 ± 0.15^{b}	45.50 ± 4.58^{b}	-20.64 ± 2.80^{b}	102.86 ± 3.65^{b}	-11.69 ± 0.97^{b}	-1.45 ± 0.10^{b}	94.08 ± 3.09^{b}	-1.86 ± 0.10^{b}
$EY_{arabinose}$	-2.58 ± 0.38^{c}	36.00 ± 8.49^{b}	-21.39 ± 0.39^{b}	101.46 ± 0.56^{b}	-14.13 ± 0.15^{cd}	-2.35 ± 0.25^{d}	92.70 ± 2.79^{b}	-2.78 ± 0.16^{c}
$EY_{xylitol}$	-2.80 ± 0.34^{c}	40.67 ± 2.31^{b}	-21.68 ± 1.77^{b}	101.70 ± 4.31^{b}	-14.31 ± 0.33^{d}	-2.06 ± 0.46^{cd}	90.99 ± 4.43^{b}	-2.74 ± 0.13^{c}
$EY_{trehalose}$	-1.90 ± 0.30^{b}	45.00 ± 2.65^{b}	-21.67 ± 1.04^{b}	101.94 ± 3.42^{b}	-12.28 ± 0.65^{b}	-1.44 ± 0.16^{b}	94.56 ± 1.66^{b}	-1.78 ± 0.13^{b}
$EY_{cellobiose}$	-2.00 ± 0.30^{b}	40.33 ± 10.41^{b}	-21.51 ± 2.07^{b}	100.21 ± 2.57^{b}	-12.33 ± 0.62^{b}	-1.63 ± 0.25^{bc}	93.84 ± 4.22^{b}	-2.05 ± 0.40^{b}
$EY_{xylooligosaccharides}$	-1.77 ± 0.15^{b}	47.67 ± 7.23^{b}	-21.28 ± 1.13^{b}	101.65 ± 5.47^{b}	-12.94 ± 1.24^{bc}	-1.50 ± 0.23^{b}	92.95 ± 4.61^{b}	-1.82 ± 0.18^{b}

Different lowercase letters indicate statistically significant differences among different egg yolk samples in the same column ($P < 0.05$).

removal of sensible heat during freezing will lead to subzero temperatures in the system until the critical mass of nuclei is reached for crystallization (Charoenrein and Harnkarnsujarit, 2017). In this stage, no ice crystals are formed because nucleation is necessary for crystallization and this temperature is termed nucleation temperature. When the system begins to nuclei, latent heat is released, leading to an abrupt increase in temperature until a maximum temperature is reached (T_{if}). One of the most crucial characteristics of frozen food systems is their freezing point, which is required for the forecasting of thermophysical properties, which are necessary to model and anticipate various technical elements of the freezing process (Rahman et al., 2009). The T_{if} of pure water is 0°C, however, it is obvious that the T_{if} of a food system is lower than 0°C, which is determined by the number of dissolved solute molecules; this phenomenon is called freezing point depression (Sviech et al., 2021). As shown in Table 1, the T_{if} of the egg yolk samples ranged from -0.97 ± 0.06°C (FEY) to -2.80 ± 0.34°C ($EY_{xylitol}$), indicating that saccharides can effectively decrease the T_{if} of egg yolks. Due to the increased mixing entropy of the smaller molecules, the presence of low-molecular-weight compounds is what primarily determines the freezing point depression of water as a colligative feature. (Sviech et al., 2021). Our previous study has confirmed that adding saccharides to egg yolks decreases the total water content (increased total solids) (Ma et al., 2023), which could lead to decreased T_{if} described in this section. Furthermore, the molecular weight of xylitol (152.146) is the second lowest in selected saccharides (L-arabinose has the lowest molecular weight, 150.13), which might explain their greatest freezing point depression phenomenon (the T_{if} of $EY_{arabinose}$ is -2.56 ± 0.38°C) (Kumar et al., 2021). Decreased partial T_{if} is often correlated to inhibited ice growth and less damage to the system (Tian et al., 2020), indicating suppressed denaturation of frozen egg yolk proteins in the presence of xylitol or L-arabinose.

Further analysis of the antigelation outcome of sugared egg yolks revealed that, as shown in Figures 1B and 1C, the addition of saccharides greatly affected the freezing curves of the samples. From 0 to −5°C, the freezing curves of the egg yolk samples flattened. At this stage, nearly 80% of the water in foods was frozen, which was termed the maximum ice crystal formation zone. Minimizing the time taken for this stage (t_z) is conducive to generating small and regular ice crystals and improving the quality of frozen food (Cen et al., 2023). In particular, the addition of saccharides decreased the t_z values (Table 1, $P < 0.05$), indicating that these saccharides could preserve the quality of frozen egg yolks, although no significant differences were detected between sugared egg yolks. $EY_{arabinose}$ had the shortest t_z (36 ± 8.49 min), which was 48% lower than that of FEY (69.33 ± 5.03 min). L-arabinose was found to be one of the active components of antifreeze polysaccharides (Zhao et al., 2022), suggesting that L-arabinose is a promising excipient for preserving the quality of frozen egg yolks. Overall, both L-arabinose and xylitol exhibited excellent regulatory effects on the freezing behaviors of egg yolks.

DSC Thermogram. DSC measurements were performed to further clarify the difference in egg yolk samples with different saccharides during freeze−thawing. The DSC thermograms of the egg yolk samples are shown in Figure 2.

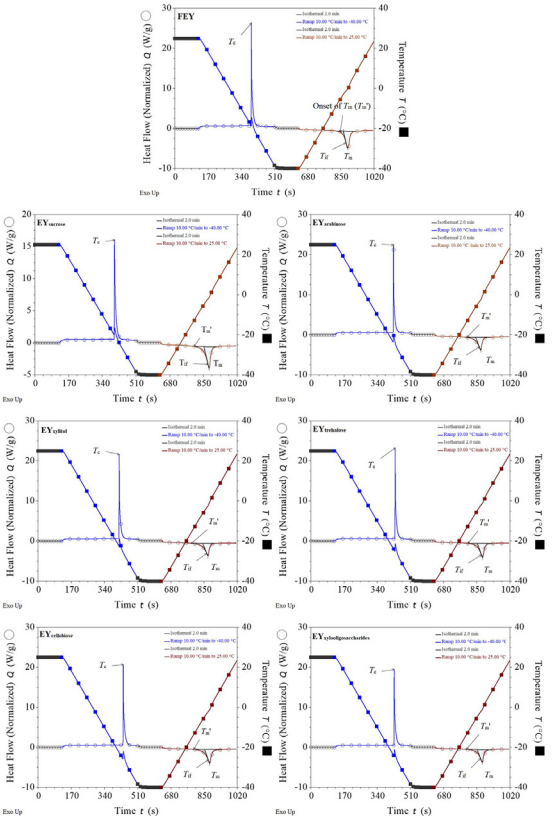

Figure 2. DSC thermograms of egg yolks.

As displayed in Figure 2, all the samples exhibited exothermic crystallization and endothermic melting peaks. The temperatures corresponding to the 2 peaks are taken as T_c and T_m respectively. Ice nucleation, ice crystal development, and recrystallization may all be influenced by altering the T_c of foods (Tian et al., 2020). In the cooling stage, we observed a small change in the temperature line, indicating a small increase in the sample temperature during cooling. This increase in sample temperature, which signals the start of ice crystallization, is caused by the self-heating of the samples during freezing (Aubuchon, 2007; Charoenrein and Harnkarnsujarit, 2017; Ma et al., 2023). FEY had the highest T_c (-16.82 ± 0.95°C, $P < 0.05$), and saccharides decreased the T_c of the egg yolks. The lowest T_c was observed for $EY_{xylitol}$ (-21.68 ± 1.77°C), although no significant differences were found between sugared egg yolks, which is consistent with previous findings (Zhu et al., 2023). Similar results were also observed for ΔH_c, where the highest ΔH_c was observed for FEY (114.41 ± 3.97 J/g, $P < 0.05$) and sugared egg yolks had comparable ΔH_c values ($P > 0.05$). Generally, decreased T_c and ΔH_c values often indicate decreased T_{if} values and less ice crystal formation (Ma et al., 2023; Zhu et al., 2023).

In the heating stage, endothermic melting peaks were observed. In the DSC thermogram (Figure 2), the peak temperature of the endotherm peak is marked as T_m, and the onset temperature of ice melting (T_m'), as its name implies, is the temperature when the ice starts to melt and is taken as the intersection point of the baseline with the left side of the endotherm. The DSC method can also be used to determine the T_{if} of food systems, and a tangent to the left side of the endothermic curve is drawn to identify the T_{if} (Syamaladevi et al., 2009). As shown in Table 1, the T_m', T_m, ΔH_m, and T_{if} values of the egg yolks exhibited similar decreasing trends with the addition of saccharides. As a unique characteristic of food products, T_m' depends on the Mw of the product (Rahman et al., 2005). A negative correlation between T_m' and the solid content has been reported by Rahman (2004) and Rahman et al. (2005), and T_m' of sugared egg yolks may increase with the increasing Mw of saccharide (Flores-Ramírez, et al., 2019). The decreased T_m values of sugared egg yolks can also be explained by the colligative freezing point depression, as indicated by the T_{if} values (Tee and Siow, 2014). The T_{if} values obtained from the DSC method were not significantly different from the T_{if} values obtained from the freezing curve ($P > 0.05$, data not shown). The ΔH_m values are often correlated with the freezable water content, and decreased ΔH_m values indicate that saccharides can decrease the freezable water content, leading to decreased ice crystal formation (Ma et al., 2023). Overall, the presence of saccharides regulated the thermal behaviors of egg yolks and inhibited the denaturation of egg yolk proteins. L-arabinose and xylitol had superior regulatory effects due to their relatively low Mw values. Considering their low caloric content, L-arabinose and xylitol are both promising excipients in sugared egg yolk formulations.

Apparent Specific Heat Capacity (C_{app}). Based on the C_{app} of foods, the specific heat during phase shift and is strongly related to the structure and energy of food, it is possible to construct frozen storage devices and analyze the thermal stresses that occur during freezing using this information (Ding et al., 2015).

As displayed in Figure 1D, the C_{app} increased dramatically with increasing temperature (approaching T_{if}), which is associated with increased melting of ice (Kumar et al., 2021). Water movement changes during phase transition, which affects its capacity to store internal energy and accounts for the variation in the C_{app} value (Kumar et al., 2018). The highest C_{app} was observed for FEY, and saccharides significantly decreased the C_{app} values; the lowest C_{app} was observed for $EY_{xylitol}$, followed by $EY_{arabinose}$. This is due to the higher water content and T_{if} of FEY, which hinder ice melting and the loss of latent heat of fusion (Kumar et al., 2021). As the egg yolks were completely melted, the C_{app} value decreased with increasing temperature because of the instantaneous loss of latent heat of fusion. Furthermore, we can see that the C_{app} values in the range of 0−20°C were greater than those in the ranges of −80°C and −20°C, presumably because water has a larger C_p value than ice (Kumar et al., 2021).

Rheological Properties of Egg Yolk Samples Subjected to Freeze–Thawing

Apparent viscosity. Liquid egg yolk is made up of a variety of biological macromolecules with different rheological properties (Zhao et al., 2024). Understanding the rheological properties of liquid egg yolks/egg yolk proteins is conducive to food engineering. The rheological performances of the egg yolk samples were observed to define their degrees of gelation. The results are shown in Figure 3A.

According to Figure 3A, both unfrozen and frozen-thawed egg yolk samples exhibited shear-thinning behaviors, where increased shear rates led to decreased apparent viscosity values, suggesting that the egg yolk samples were non-Newtonian (pseudoplastic) fluids. Most non-Newtonian fluids possess the characteristic of a molecular chain structure, which tends to orient in planes of maximal tension resulting in a decrease in viscosity with increasing velocity gradient (Van Canneyt and Verdonck, 2014). Interestingly, unfrozen FEY had low initial-shear-rate apparent viscosity values (below 3.75 Pa·s), and the addition of saccharides further decreased the apparent viscosity of the egg yolks. Saccharides have also been reported to decrease the viscosity of batters and dough (Figoni, 2010). Saccharides are hygroscopic to some extent, indicating that they can attract and bond to water (Figoni, 2010). Water molecules were drawn away from egg yolk particles in the presence of saccharides, which also increased the amount of free (bulk) water in suspension and decreased the

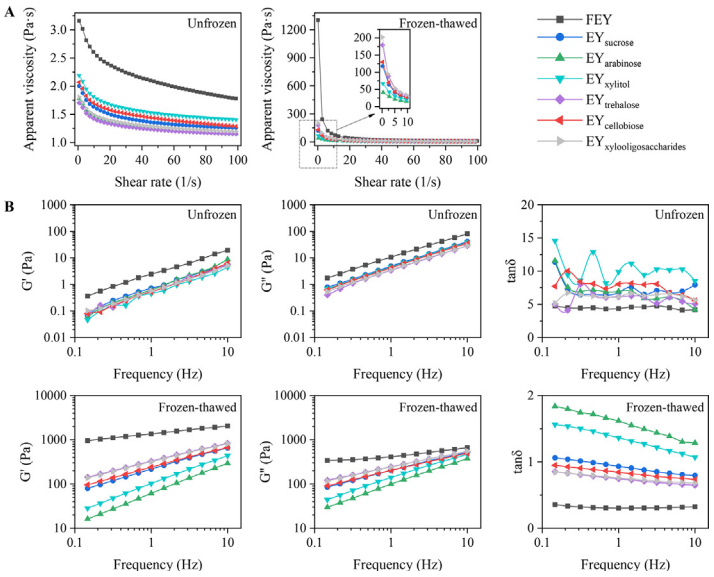

Figure 3. Changes in the apparent viscosity (A) and viscoelasticity (B) of unfrozen and frozen-thawed egg yolks.

amount of physically connected water (thick water layer) (Falkowski and Szafran, 2016). A fluid flows easily and is deemed thin if its molecules or particles can easily pass through one another (Figoni, 2010), which might explain the relatively lower apparent viscosity of sugared egg yolks. In addition, viscosity is a function of the internal friction of a fluid under force (Van Canneyt and Verdonck, 2014), and it was inferred that saccharides decreased the internal friction of egg yolks before freezing. This finding agrees with our results regarding the molecular interactions in sugared egg yolks; saccharides decreased the molecular forces between egg yolk proteins before freezing.

After the egg yolk samples were freeze–thawed, their apparent viscosity drastically increased. The frozen-thawed FEY had the highest initial-shear-rate apparent viscosity (1,302.26 Pa·s), indicating severe gelation. The apparent viscosity of frozen-thawed sugared egg yolks ranged from 41 to 203 Pa·s, indicating that the gelation of frozen-thawed egg yolk samples was regulated to various degrees with the addition of saccharides. To further quantify the flow behaviors of the egg yolk samples, a powder-law equation was used to fit the apparent viscosity and shear rate data. The parameters obtained from the model are shown in Table 2.

The consistency index K provides information on the viscosity of the fluid, and the flow behavior index n indicates the degree of structuring of the sample (Ma et al., 2021). The sugared egg yolk samples exhibited significantly lower K values and significantly higher n values than FEY ($P < 0.05$), which can be attributed to the hygroscopic and protein-stabilizing nature of saccharides (Figoni, 2010; Zhu et al., 2021). Lower K values indicate less viscous samples, and higher n values indicate less structured samples. Among the unfrozen samples, the lowest K value was observed for the $EY_{trehalose}$ samples (1.770 ± 0.162 Pa·s^n). Trehalose may be more hydrating and easier to replenish water molecules surrounding proteins (Wang et al., 2023), yet there was no discernible difference between $EY_{sucrose}$, $EY_{arabinose}$, and $EY_{trehalose}$ ($P > 0.05$). The type of saccharides did not appear to have a major impact on the fluidity of the sugared egg yolk samples before freezing, as evidenced by the lack of significant differences observed between the n values of the unfrozen sugared egg yolk samples.

However, after the egg yolk samples were freeze–thawed, a tremendous increase in the K value was observed ($P < 0.001$), indicating a sharp increase in the viscosity of the frozen-thawed samples. In addition, the n values exhibited the opposite decreasing trend, suggesting that freeze–thaw treatment led to more structured egg yolk samples with less fluidity. Freeze-induced protein denaturation may result in the formation of protein aggregates with higher Mw and less solubility (Tian, et al., 2022). It is believed that the viscosity of egg yolks may be influenced by the Mw of the dispersed phase in terms of the molecular length and degree of aggregation (Wang et al., 2021a). The sugared egg yolk samples exhibited significantly lower K values and significantly greater n values than FEY, even after freeze–thawing treatment ($P < 0.05$). All of these results confirmed the gelation behaviors of frozen-thawed egg yolks, but the presence of saccharides alleviated the degree of gelation. The thermal properties described previously indicated that saccharides could decrease the T_{if} and ΔH_m of egg yolks, thus leading to limited ice crystal formation. Small ice crystals cause less damage to protein molecules and the unfolding of protein molecules is limited. The molecular chains were less entangled and had a limited molecular length. The lowest K values were detected for the $EY_{arabinose}$ samples (36.447 ± 1.202 Pa·s^n), and no significant differences were detected between $EY_{arabinose}$ and $EY_{xylitol}$ ($P > 0.05$). The n values suggested that $EY_{arabinose}$ had the best fluidity, followed by $EY_{xylitol}$. The remaining sugared egg yolk samples exhibited comparable fluidity, indicating that L-arabinose and xylitol were more effective at regulating the gelation of frozen-thawed egg yolks. L-arabinose was

Table 2. Power-law equation parameters of egg yolk samples regarding viscosity.

	Unfrozen samples			Frozen-thawed samples		
	K / Pa·s^n	n	r	K / Pa·s^n	n	r
FEY	3.349 ± 0.141^{a}	0.868 ± 0.005^{b}	0.987	$353.367 \pm 28.217^{A, ***}$	$0.318 \pm 0.014^{D, ***}$	0.987
$EY_{sucrose}$	1.966 ± 0.142^{bc}	0.900 ± 0.011^{a}	0.984	$76.187 \pm 2.623^{B, ***}$	$0.508 \pm 0.001^{C, ***}$	0.951
$EY_{arabinose}$	1.941 ± 0.081^{bc}	0.898 ± 0.005^{a}	0.994	$36.447 \pm 1.202^{C, ***}$	$0.544 \pm 0.003^{A, ***}$	0.962
$EY_{xylitol}$	2.187 ± 0.124^{b}	0.895 ± 0.001^{a}	0.993	$53.967 \pm 0.555^{C, ***}$	$0.534 \pm 0.003^{B, ***}$	0.957
$EY_{trehalose}$	1.770 ± 0.162^{c}	0.901 ± 0.009^{a}	0.994	$93.383 \pm 2.817^{B, ***}$	$0.503 \pm 0.003^{C, ***}$	0.944
$EY_{cellobiose}$	2.165 ± 0.233^{bc}	0.889 ± 0.004^{a}	0.990	$81.167 \pm 6.475^{B, ***}$	$0.505 \pm 0.007^{C, ***}$	0.948
$EY_{xylooligosaccharides}$	1.933 ± 0.069^{b}	0.879 ± 0.006^{a}	0.996	$95.493 \pm 8.509^{B, ***}$	$0.498 \pm 0.005^{C, ***}$	0.947

Different lowercase letters indicate statistically significant differences among unfrozen samples (0 d) within the same column ($P < 0.05$); different uppercase letters indicate statistically significant differences among frozen-thawed samples (3 d) within the same column ($P < 0.05$); *** indicates statistically significant differences between the same parameter of unfrozen and frozen-thawed samples within the same row ($P < 0.001$).

found to be most effective at decreasing t_z values, and xylitol was effective at decreasing the T_{if} of egg yolks. Therefore, ice crystals caused less damage in the $EY_{arabinose}$ and $EY_{xylitol}$ samples. Furthermore, our previous study on the aggregation rate of frozen-thawed egg yolk samples also indicated that $EY_{arabinose}$ and $EY_{xylitol}$ had low aggregation rates during freezing (Ma et al., 2023). In addition, large saccharide molecules have been reported to have an inferior protein stabilizing effect due to steric hindrance, and insufficient water-substituting interactions with proteins can occur (Izutsu, 2018). Among the tested saccharides, L-arabinose and xylitol had the lowest Mw values (150.13 and 152.146, respectively), which explains their exceptional gelation-regulating effects over the other saccharides used in this study.

Viscoelasticity. Based on the structural characteristics of foods, semisolid foods can be either viscoelastic solids or fluids, while the majority of fluid foods exhibit a relatively high proportion of viscous to elastic behavior (Zheng, 2019). In our case, the egg yolk samples prepared in our study were either fluids or semisolids; therefore, investigating their viscoelastic behaviors can help us to better understand their physical properties. The viscoelasticity results are shown in Figure 3B.

The elastic (solid-like) behavior of materials is represented by the storage modulus (G'), whereas the viscous (fluid-like) behavior is represented by the loss modulus (G'') (Zheng, 2019). Viscoelastic solids, which are elastic-dominant materials, have tan δ values less than 1, whereas viscoelastic fluids, which are viscous-dominant materials, have tan δ values greater than 1. According to Figure 3B, for the unfrozen samples, all the G'' values surpassed the G' values, indicating that the unfrozen samples exhibited more viscosity than elasticity. All *tan* δ values greater than 1 also confirmed that the unfrozen samples were viscous-dominant materials, and the lowest tan δ values were observed for FEY ($P < 0.05$).

After freeze–thawing, the modulus patterns of the samples changed significantly. Most samples (excluding $EY_{arabinose}$ and $EY_{xylitol}$) exhibited higher G' values than G'' values (*tan* $\delta < 1$), suggesting that most egg yolks were viscoelastic solids after freeze–thawing. $EY_{arabinose}$ and $EY_{xylitol}$ were the only 2 samples exhibiting *tan* $\delta > 1$, which in turn confirmed our results of apparent viscosity.

To further investigate the structured degree of egg yolk samples, the obtained G' and G'' values were used to calculate the complex modulus (G^*) (data not shown). G^* is regarded as a measure of the general rigidity of semisolid foods, and was subsequently fitted with a power law equation (Gabriele et al., 2001; Zheng, 2019). The results of the fitting are presented in Table 3. The decreased A_F values of the sugared egg yolk samples compared to those of the FEY samples can be attributed to their weakened structure. However, the nearly unchanged z values among the unfrozen egg yolk samples suggested that the saccharide type did not have a significant effect on the extension of the egg yolk samples.

After the egg yolks were freeze–thawed, all the A_F and z values increased significantly ($P < 0.001$), suggesting that interactions between rheological units became stronger and more correlated in the 3-dimensional

Table 3. Power-law equation parameters of egg yolk samples regarding viscoelasticity.

	Unfrozen samples			Frozen-thawed samples		
	A / Pa·s$^{1/z}$	z	r^2	A / Pa·s$^{1/z}$	z	r^2
FEY	11.072 ± 0.198^{a}	1.142 ± 0.008^{a}	0.999	$1428.885 \pm 25.768^{A, ***}$	$5.556 \pm 0.062^{A, ***}$	0.999
$EY_{sucrose}$	4.948 ± 0.181^{b}	1.081 ± 0.017^{c}	0.999	$298.218 \pm 0.175^{C, ***}$	$2.195 \pm 0.007^{D, ***}$	0.999
$EY_{arabinose}$	4.416 ± 0.039^{b}	1.078 ± 0.003^{c}	0.999	$117.669 \pm 5.127^{D, ***}$	$1.637 \pm 0.003^{F, ***}$	0.999
$EY_{xylitol}$	4.551 ± 0.030^{b}	1.076 ± 0.007^{c}	0.999	$174.343 \pm 2.352^{D, ***}$	$1.757 \pm 0.003^{E, ***}$	0.999
$EY_{trehalose}$	3.493 ± 0.081^{c}	1.076 ± 0.012^{c}	0.999	$409.247 \pm 5.782^{B, ***}$	$2.580 \pm 0.037^{B, ***}$	0.999
$EY_{cellobiose}$	4.415 ± 0.952^{b}	1.093 ± 0.024^{bc}	0.999	$313.815 \pm 4.605^{C, ***}$	$2.336 \pm 0.005^{C, ***}$	0.999
$EY_{xylooligosaccharides}$	3.711 ± 0.140^{c}	1.115 ± 0.011^{b}	0.999	$400.629 \pm 8.686^{B, ***}$	$2.538 \pm 0.026^{B, ***}$	0.999

Different lowercase letters indicate statistically significant differences among unfrozen samples (0 d) within the same column ($P < 0.05$); different uppercase letters indicate statistically significant differences among frozen-thawed samples (3 d) within the same column ($P < 0.05$); *** indicates statistically significant differences between the same parameter of unfrozen and frozen-thawed samples within the same row ($P < 0.001$).

structure of the egg yolk samples after freeze–thaw treatment. Our results regarding the intermolecular forces maintaining the egg yolk lipoprotein matrix also confirmed that the interactions between egg yolk particles were intensified after freeze–thaw treatment. Frozen-thawed FEY undoubtedly had the highest A_F and z values (1428.885 Pa·s$^{1/z}$ and 5.556, respectively), and the addition of saccharides contributed to the weak network of sugared egg yolk samples. Although the A_F values of $EY_{arabinose}$ and $EY_{xylitol}$ were not significantly different (same strength), a significant difference was found in the network extension, as manifested by the relatively lower apparent viscosity of $EY_{arabinose}$ compared to that of $EY_{xylitol}$.

Structural Properties of Egg Yolk Samples Subjected to Freeze–Thawing

Molecular Interactions. Intermolecular (cohesive) forces play a crucial role in fluid viscosity (Sahin and Sumnu, 2006). Protein aggregation and gelation are controlled by intermolecular force balances (Wang et al., 2020). To determine how saccharides influence the viscosity of unfrozen egg yolks and the aggregation/gelation behaviors of frozen-thawed egg yolk proteins, we investigated the intermolecular forces involved in egg yolk samples using 3 shielding agents, NaCl, SDS, and urea. NaCl can cause protein molecules to repel each other electrostatically, SDS can shield hydrophobic interactions, and urea can eliminate hydrogen bonding (Wang et al., 2020; Wang et al., 2021b). The intermolecular forces involved in unfrozen and frozen-thawed egg yolk samples are shown in Figure 4.

As shown in the figure, protein solubility was the highest in the presence of SDS, followed by that in the presence of NaCl and urea. Saccharide addition decreased the intermolecular forces of egg yolk proteins before freezing, thus explaining the reduced viscosity of unfrozen sugared egg yolk samples compared to that of unfrozen FEY. The viscosity of a liquid is a function of the intermolecular forces that restrict molecular motion (Sahin and Sumnu, 2006). The decrease in intermolecular forces because of the addition of saccharides may

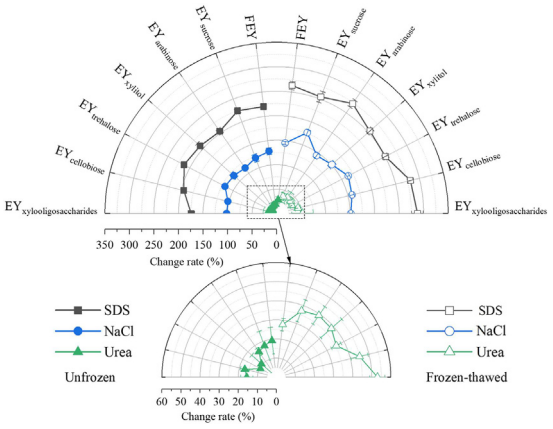

Figure 4. Changes in the intermolecular forces of unfrozen and frozen-thawed egg yolk proteins.

have promoted the molecular motion of the egg yolk particles, thus decreasing the viscosity.

After the egg yolk samples were freeze–thawed, protein solubility increased significantly in the presence of shielding agents ($P < 0.001$), especially SDS, indicating intensified molecular interactions. The formation of ice crystals during freezing can damage protein integrity, exposing more hydrophobic groups. Hydrophobic interactions were dominant in freezing-induced egg yolk gelation; additionally, strong LDL-granule interactions driven by hydrophobic interactions were observed in frozen-thawed egg yolks (Au et al., 2015; Primacella et al., 2018; Wang et al., 2021b).

As described in the Introduction, whole egg yolks can be fractionated into plasma (supernatant) and granules (sediment) via moderate centrifugation. The insoluble granules are assembled from HDLs and phosvitin via phosphocalcic bridges (Anton, 2007). SDS works as an effective protein denaturant by eliminating hydrophobic interactions between proteins; it can dissolve all egg yolk proteins, including apo-HDL and apo-LDL (Wang et al., 2022), leading to the highest extraction of egg yolk protein content, as observed in this study. Furthermore, the self-assembly of egg yolk granules is primarily governed by attractive phosphocalcic bridges and repulsive electrostatic interactions (Li et al., 2022). In contrast, NaCl dissolves yolk granules with ionic strengths greater than 0.3 mol/L at neutral pH (Anton, 2007). In this study, 1% NaCl (0.17 mol/L) could only partially dissolve yolk granules, which explains the relatively lower protein change rate in the presence of NaCl. Usually, 8 mol/L urea is used to eliminate hydrogen bonds between proteins. The screening of intramolecular hydrogen bonds, including hydrogen bonds with polar protein moieties (in particular peptide groups), is triggered by direct contact with urea (Bennion and Daggett, 2003). Additionally, high urea concentrations affect protein stability (Zou et al., 1998). Therefore, we used only 1 mol/L urea in our study. Although the rate of change in protein solubility in urea-treated egg yolks was the lowest, its value increased considerably after freeze–thawing.

Following the freeze−thawing of egg yolk samples, an increase in intermolecular interactions between egg yolk proteins was observed in the presence of saccharides; the egg yolk samples exhibited less aggregation or gelation than FEY after freeze–thawing. Similar results were also observed in −18°C and −40°C-treated egg yolks (Wang, et al., 2021b). The authors reported that egg yolks frozen at −40°C exhibit less gelation behavior than those frozen at −18°C; however, −40°C-treated egg yolks exhibit an increase in the rate of change in protein solubility in the presence of these 3 shielding agents. We believe that more in-depth studies should be performed to further elucidate this issue.

Aggregation Characteristics. Visual observation provides intuitive information on the appearance of egg yolks. CLSM and particle size distribution (**PSD**) have been widely used to characterize protein aggregation in egg yolk proteins (Wang et al., 2021a; Wang et al.,

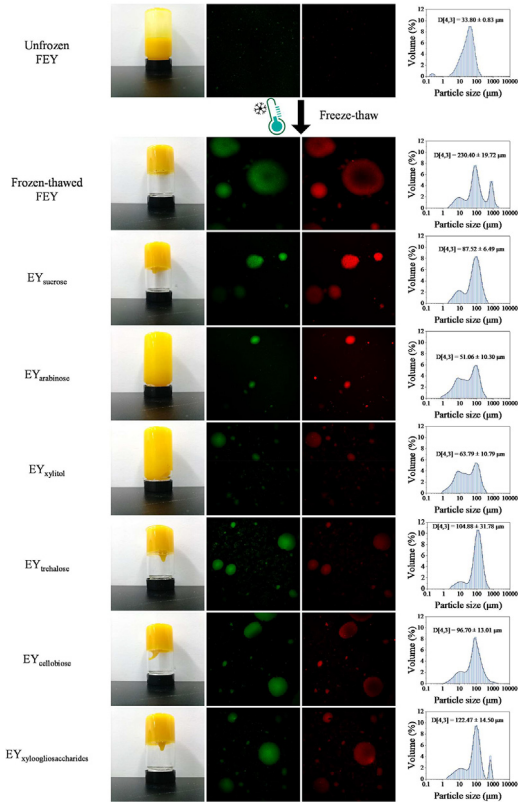

Figure 5. Changes in the macro-appearance, micro-appearance, and PSD of frozen-thawed egg yolks.

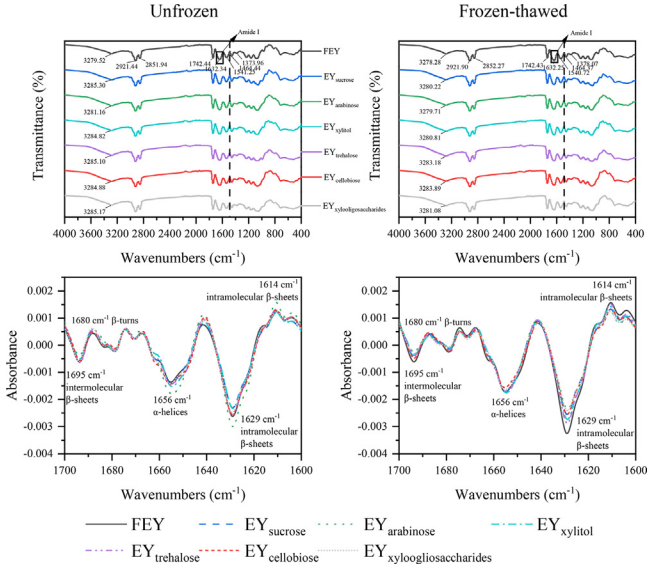

Figure 6. Changes in FTIR spectra and secondary structure of unfrozen and frozen-thawed egg yolk proteins (freeze-dried samples).

2023). Our turbidity results indicated that the aggregation behavior of the unfrozen egg yolk proteins was not sufficiently distinct (Ma et al., 2023), in this section, only unfrozen FEY and frozen-thawed egg yolk samples were involved. Visual observation, CLSM, and PSD of egg yolk samples are shown in Figure 5.

The unfrozen FEY had good fluidity; after freeze–thawing, only $EY_{arabinose}$ and $EY_{xylitol}$ exhibited fluidity; however, many remained on the wall of the vial, indicating increased viscosity. Other samples had poor fluidity, which was consistent with the apparent viscosity data. For CLSM observation, proteins were stained with Nile blue, which is shown in green, while lipids were stained with Nile red, which is shown in red. The unfrozen FEY exhibited vague signals in the CLSM images, with a volume average particle diameter (D [4,3]) of 33.80 ± 0.83 μm. After freeze–thawing, all samples showed aggregation, suggesting that freeze–thaw treatment led to the unfolding of egg yolk proteins and favored protein aggregation. The aggregates gave strong signals in the CLSM images. The PSD of the frozen-thawed samples shifted to larger particle sizes, which also confirmed aggregation. Frozen-thawed FEY had the largest D [4,3] value ($P < 0.05$), and $EY_{arabinose}$ had the smallest D [4,3] value, followed by $EY_{xylitol}$, which is consistent with our results on turbidity (Ma et al., 2023). As reported, saccharides can replace the water molecules that normally surround protein surfaces, thereby maintaining the protein structure during freezing (Tian et al., 2022). Therefore, the sugared egg yolk samples formed smaller aggregates after freeze–thawing. Furthermore, particle size has been reported to have effects on the material properties of egg yolks, such as viscosity (Primacella et al., 2018). The decreased particle size and weaker aggregation may have contributed to the decreased apparent viscosity and increased viscous behavior of egg yolk samples after freeze–thawing.

FTIR Spectrum and Secondary Structure. Protein denaturation involves changes in its secondary and tertiary structures by breaking bonds and interactions that stabilize the protein conformation (Charoenrein and Harnkarnsujarit, 2017). FTIR spectroscopy has emerged as a useful tool for characterizing the functional groups of biological molecules and the secondary structure of proteins (Uysal and Boyaci, 2020; Qing, et al., 2023). The FTIR spectra are shown in Figure 6.

According to Figure 6, the spectra of the egg yolk samples exhibited a series of characteristic peaks at several wavenumber ranges. The stretching of O−H and N−H vibrations was found in the range of 3,700 to 3,000/cm, which is attributed to the water molecules at the protein−lipid interface remaining within egg yolk particles after lyophilization and the Amide A band of proteins coupled with hydrogen bonding (Krilov et al., 2009). A bathochromic shift of this band was found between the FEY and the sugared egg yolk samples; a hypsochromic shift was found between the unfrozen and frozen-thawed samples. The presence of hydroxyl groups in saccharides could lead to a shift to higher wavenumbers (Fuertes et al., 2017). Furthermore, freeze–thaw treatment intensified the hydrogen bonding of egg yolk samples, and the band moved to lower wavenumbers when a protein's N−H group was involved in hydrogen bonding (Nagarajan et al., 2012). The bands appearing at 2,921/cm and 2,852/cm can be assigned to the C−H stretching vibrations from lipid chains (both asymmetric and symmetric) (Krilov, et al., 2009; Uysal and Boyaci, 2020). The band at 1,742/cm is attributed to C = O stretching from ester bonds in phospholipids (Krilov et al., 2009). The broad band between 1,700 and 1,600/cm

is the Amide I band, which mainly contains C=O stretching vibrations of protein peptide bonds; the band between 1,600 and 1,500/cm is the Amide II band, which is mainly caused by C−N stretching vibrations and N−H deformation of protein peptides (Liu et al., 2023a). The former is more frequently used to analyze protein secondary structures, which will be discussed later. The band at 1,467/cm is attributed to the bending vibrations of the CH_2 groups in the acyl chains of lipids. The adjacent band on the right is the composite band corresponding to the symmetric bending of CH_3 groups at 1,378/cm and the CH_2 wagging vibration at 1,367/cm (Krilov, et al., 2009). In addition, 3 lipid-associated bands could be observed in the approx. 1,234, 1,162, and 1,085/cm regions (Fuertes, et al., 2017).

The Amide I region (1,700−1,600/cm) of the FTIR spectrum is the most beneficial for determining the secondary structure of proteins. Figure 6 presents the second-derivative spectra of the Amide I region of the egg yolk samples. Five prominent peaks can be found in the figure. Two distinct peaks were observed at 1,656/cm and 1,629/cm, which are assigned to α-helices and intramolecular β-sheets of proteins, respectively (Liu et al., 2023a), indicating that the secondary structure of egg yolk proteins is dominated by α-helices and intramolecular β-sheets. Regarding the α-helices of the unfrozen egg yolk samples, the intensity at 1,656/cm exhibited an increasing trend between the FEY and sugared egg yolk samples, indicating that the lyophilized sugared egg yolk samples had more α-helix structures than FEY. We believe that pretreating unfrozen egg yolk samples with lyophilization played a role and that protein denaturation occurred in the unfrozen samples. When the temperature decreased below the T_{if} of egg yolks, the water inside the egg yolks expanded and formed ice crystals, which damaged protein integrity, as manifested by changes in protein structure. In other words, the α-helix of egg yolk proteins was preserved to various degrees during lyophilization in the presence of saccharides since the presence of saccharides decreased the T_{if} of egg yolks. Similar results were reported by Wang et al. (2023), who investigated the effect of disaccharides on egg yolk lipoprotein structure during lyophilization. $EY_{arabinose}$ had the highest α-helix content, followed by $EY_{xylitol}$, indicating that L-arabinose was the most effective in preserving the secondary structure of egg yolk proteins and that the least protein denaturation was detected. This finding is consistent with our data on rheology and aggregation behavior. The conversion from α-helices to β-sheets of proteins after freezing has also been observed by many scholars (Wang et al., 2020). In our case, fewer α-helical structures of egg yolk samples were involved in such a conversion; therefore, a decrease in intensity at 1656 cm^{-1} corresponding to intramolecular β-sheets was observed for egg yolk samples.

For frozen-thawed egg yolks, we believe that these samples may be regarded as those subjected to 2 freeze–thaw cycles since 2 freezing processes were involved. By comparing unfrozen FEY and frozen-thawed samples, the intensity at 1,656/cm increased, indicating increased α-helix content. Li et al. (2018) also reported that the α-helix content of egg yolk proteins exhibited an overall increasing trend during 0−9 freeze–thaw cycles. However, the α-helix content of frozen-thawed egg yolk samples did not increase as much as that of FEY, further supporting the cryoprotective effect of saccharides. Although L-arabinose and xylitol were less effective in frozen-thawed samples, we believe our results regarding unfrozen samples may be more applicable in the practical production of frozen egg yolks since frozen egg yolk (as a product) is suggested to be consumed within 3 d once thawed, and freeze–thaw cycles are highly unrecommended.

Intrinsic Fluorescence Spectra and Tertiary Structure. Intrinsic fluorescence spectroscopy is a common and useful tool to evaluate changes in the tertiary structure of proteins, mainly by monitoring the microenvironment of tryptophan (**Trp**) (Ma et al., 2022; Liu, et al., 2023c). The indole group of Trp absorbs near 280 nm, and emits near 340 nm; the emission spectrum of indole is highly sensitive to solvent polarity, which can be used as an indicator of the folded and unfolded state of proteins in solutions (Lakowicz, 2006a). The intrinsic fluorescence spectra of the samples are shown in Figure 7.

Among the unfrozen samples, FEY had the highest maximum fluorescence intensity ($\mathbf{FI_{max}}$) (3,722 ± 66), and the addition of saccharides decreased the FI_{max} of the egg yolks (ranging from 2,479 to 3,116). We believe this could be attributed to saccharide-induced fluorescence quenching of Trp residues in proteins (Das et al., 2017; Kong et al., 2020). Our previous study indicated that saccharides could molecularly contact the protein surface (Ma et al., 2023). Upon contact, the fluorophore returned to the ground state without photon emission, and quenching occurred (Lakowicz, 2006c). This observation indicated that some of the Trp residues existed on the protein surface; if all the Trp residues were buried inside the protein, quenching was not expected to occur (Lakowicz, 2006b). The values of the wavenumbers

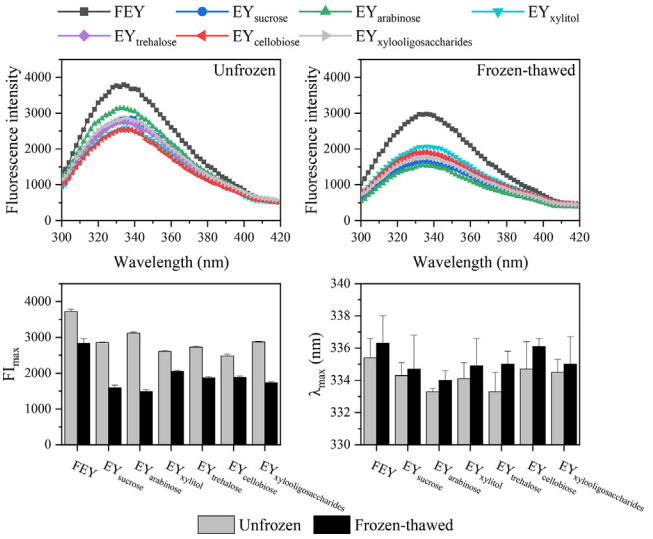

Figure 7. Changes in the intrinsic fluorescence spectra, FI_{max}, and λ_{max} of unfrozen and frozen-thawed egg yolk proteins.

corresponding to FI_{max} ($\boldsymbol{\lambda_{max}}$) were all greater than 330 nm, which also indicated that the Trp residues of the proteins were mostly assigned to an overall polar environment (Vivian and Callis, 2001). Furthermore, the λ_{max} of the samples exhibited a slight hypsochromic shift with saccharide addition (from 335.4 to 333.3 nm), and the λ_{max} shifted toward lower wavelengths, indicating that the environment of the Trp residues became hydrophobic (Ma et al., 2022). This could result from the compaction effect of saccharides on protein conformation (Das et al., 2017), which can decrease the particle size of protein molecules (data not shown) and cause internal Trp residues to become relatively more buried, thus leading to decreased λ_{max} values. The compact state of proteins is conducive to withstanding unfolding and denaturation, and the presence of saccharides is indispensable.

After the egg yolks were freeze–thawed, the FI_{max} of the egg yolks further decreased. Unlike the saccharide-induced decrease in FI_{max}, this decrease in FI_{max} of the samples indicated that the proteins were unfolded due to freeze-induced denaturation (Wang et al., 2021a). During freezing, water was gradually converted to ice crystals, accompanied by an increase in system volume; due to the restriction of the container, a hump in frozen egg yolks (without thawing) was observed (data not shown), which can be caused by the extrusion of ice crystals. The expanded ice crystals could cause physical damage to protein molecules, which were forced to unfold and denature. A bathochromic shift was observed in the λ_{max} of the samples after freeze–thawed. This indicated that the buried Trp residues were exposed to a hydrophilic environment, that is, the Trp residues were more exposed to the solvent. As discussed above, the presence of saccharides could decrease the vulnerability of proteins to freeze-induced unfolding and denaturation. Furthermore, the thermal properties of the samples indicated that the sugared egg yolks tended to have smaller ice crystals, thus leading to limited expansion of protein molecules. $EY_{arabinose}$ had the lowest λ_{max} value, indicating that L-arabinose can effectively inhibit the unfolding of egg yolk proteins caused by freeze–thawing, which agrees with our previously described findings.

CONCLUSIONS

In this study, saccharides were used to regulate the gelation behaviors of egg yolks by monitoring their thermal, rheological, and structural properties. The results showed that saccharides could shorten the t_z and decrease the T_{if}, ΔH, and C_{app} values of egg yolks, indicating limited ice crystal formation in these samples, which is related to the Mw of the additive saccharides. Rheological analyses revealed that L-arabinose and xylitol were able to maintain the viscous behavior of frozen-thawed egg yolks, which can be attributed to controlled aggregation and a decreased degree of protein structural changes. Saccharides can contact the protein surface to replace partial water molecules accessible to the protein surface and enhance the compactness of proteins to withstand freeze-induced unfolding and denaturation. Saccharides themselves can also attract water molecules and hinder the growth of large ice crystals. Overall, low-molecular-weight and low-calorie L-arabinose and xylitol have great potential for replacing sucrose in frozen egg yolk formulas. We hope that our findings can be used to develop new egg yolk products, optimize processing conditions, and inhibit the gelation behaviors of frozen egg yolks.

ACKNOWLEDGMENTS

The authors gratefully acknowledge the financial support provided by the National Natural Science Foundation of China [grant number: 31972098] and the China Agriculture Research System of MOF and MARA [grant number: CARS-40].

DISCLOSURES

The authors declare no conflicts of interest.

REFERENCES

Ankita, and A. K. Nain. 2020. Study of solvation behaviour and interactions of drug betaine hydrochloride in aqueous-D-xylose/L-arabinose solutions at different temperatures by using volumetric, acoustic and viscometric methods. J. Chem. Thermodynamics 143:106046.

Anton, M. 2007. Composition and structure of hen egg yolk. *Bioactive Egg Compounds*. R. Huopalahti, R. López-Fandiño, M. Anton and R. Schade, eds. Springer, Berlin, Heidelberg. 1–6.

Anton, M. 2013. Egg yolk: structures, functionalities and processes. J. Sci. Food Agric. 93:2871–2880.

Au, C., N. C. Acevedo, H. T. Horner, and T. Wang. 2015. Determination of the gelation mechanism of freeze-thawed hen egg yolk. J. Agric. Food Chem. 63:10170–10180.

Aubuchon, S. R. 2007. Interpretation of the crystallization peak of supercooled liquids using Tzero® DSC. https://www.tainstruments.com/pdf/literature/TA344%20Crystallization%20Peak%20of%20Supercooled%20Liquids%20by%20Tz%20DSC.pdf. Accessed Mar. 16 2023.

Bennion, B. J., and V. Daggett. 2003. The molecular basis for the chemical denaturation of proteins by urea. Proc. Natl. Acad. Sci. 100:5142–5147.

Cen, K., C. Huang, X. Yu, C. Gao, Y. Yang, X. Tang, and X. Feng. 2023. Quinoa protein pickering emulsion: a promising cryoprotectant to enhance the freeze-thaw stability of fish myofibril gels. Food Chem. 407:135139.

Charoenrein, S., and N. Harnkarnsujarit. 2017. Chapter 2 - Food freezing and non-equilibrium states. Pages 39–62 in Non-equilibrium States and Glass Transitions in Foods. B. Bhandari and Y. H. Roos, eds. Woodhead Publishing, Cambridge.

Chi, Y., and Z. Ma. 2023. Egg yolk lipid and protein functionality. Pages 161–174 in Handbook of Egg Science and Technology. Y. Mine, V. Guyonnet, H. Hatta, F. Nau and N. Qiu, eds. CRC Press, Boca Raton.

Das, A., P. Basak, R. Pattanayak, T. Kar, R. Majumder, D. Pal, A. Bhattacharya, M. Bhattacharyya, and S. P. Banik. 2017. Trehalose induced structural modulation of Bovine Serum Albumin at ambient temperature. Int. J. Biol. Macromol. 105:645–655.

Ding, X., H. Zhang, L. Wang, H. Qian, X. Qi, and J. Xiao. 2015. Effect of barley antifreeze protein on thermal properties and water state of dough during freezing and freeze-thaw cycles. Food Hydrocoll. 47:32–40.

Falkowski, P., and M. Szafran. 2016. Role of molecular structure of monosaccharides on the viscosity of aqueous nanometric alumina suspensions. Ceram. Int. 42:8572–8580.

Fei, T., F. M. A. Leyva-Gutierrez, Z. Wan, and T. Wang. 2021. Gelation inhibiting additives and freezing impact rheological, thermal, and microstructural properties of yolk. LWT 144:111160.

Figoni, P. I. 2010. Sugar and other sweeteners. *How Baking Works: Exploring the Fundamentals of Baking Science*. John Wiley & Sons, Hoboken, New Jersey, 163–212.

Flores-Ramírez, A. J., P. García-Coronado, A. Grajales-Lagunes, R. G. García, M. A. Archila, and M. A. Ruiz Cabrera. 2019. Freeze-concentrated phase and state transition temperatures of mixtures of low and high molecular weight cryoprotectants. Adv. Polymer Technol. 2019:5341242.

Fuertes, S., A. Laca, P. Oulego, B. Paredes, M. Rendueles, and M. Díaz. 2017. Development and characterization of egg yolk and egg yolk fractions edible films. Food Hydrocoll. 70:229–239.

Gabriele, D., B. de Cindio, and P. D'Antona. 2001. A weak gel model for foods. Rheol. Acta 40:120–127.

Izutsu, K.i. 2018. Applications of freezing and freeze-drying in pharmaceutical formulations. Pages 371-383 in Survival Strategies in Extreme Cold and Desiccation: Adaptation Mechanisms and Their Applications. M. Iwaya-Inoue, M. Sakurai and M. Uemura, eds. Springer, Singapore.

Kong, F., S. Kang, J. Tian, M. Li, X. Liang, M. Yang, Y. Zheng, Y. Pi, X. Cao, Y. Liu, and X. Yue. 2020. Interaction of xylitol with whey proteins: Multi-spectroscopic techniques and docking studies. Food Chem. 326:126804.

Krilov, D., M. Balarin, M. Kosović, O. Gamulin, and J. Brnjas-Kraljević. 2009. FT-IR spectroscopy of lipoproteins—a comparative study. Spectrochimica Acta Part A 73:701–706.

Krishna Kumar, P., K. Bhunia, J. Tang, B. A. Rasco, P. S. Takhar, and S. S. Sablani. 2018. Thermal transition and thermo-physical properties of potato (*Solanum tuberosum L.*) var. Russet brown. J. Food Measure. Characterization 12:1572–1580.

Kumar, P. K., A. Parhi, and S. S. Sablani. 2021. Development of high-fiber and sugar-free frozen pancakes: Influence of state and phase transitions on the instrumental textural quality of pancakes during storage. LWT 146:111454.

Introduction to fluorescence. (2006a). Pages 1−26 in Principles of Fluorescence Spectroscopy. J. R. Lakowicz and J. R. Lakowicz, eds. Springer, Boston, MA.

Protein fluorescence. (2006b). Pages 529−575 in Principles of Fluorescence Spectroscopy. J. R. Lakowicz and J. R. Lakowicz, eds. Springer, Boston, MA.

Quenching of fluorescence. (2006c). Pages 277−330 in Principles of Fluorescence Spectroscopy. J. R Lakowicz and J. R. Lakowicz, eds. Springer, Boston, MA.

Li, M., X. Li, J. Li, M. Lu, X. Liu, and X. Duan. 2018. Effects of multiple freeze−thaw treatments on physicochemical and biological activities of egg phosvitin and its phosphopeptides. Food Funct. 9:4602–4610.

Li, T., H. Su, J. Zhu, and Y. Fu. 2022. Janus effects of NaCl on structure of egg yolk granules. Food Chem. 371:131077.

Li, X., Q. Huang, Y. Zhang, X. Huang, Y. Wu, F. Geng, M. Huang, P. Luo, and X. Li. 2023. Inhibitory mechanism of trypsin combined with d-galactose on freeze-induced gelation and the physicochemical and protein properties of egg yolk. LWT 188:115337.

Liu, L., J. Bi, Y. Chi, and Y. Chi. 2024. Mechanism of amino acid delay on thermal aggregation behavior of liquid egg yolk: thermal aggregation, water distribution, molecular structure. Food Hydrocoll. 148:109453.

Liu, Y., Y. Chi, and Y. Chi. 2023a. Effects of $CaCl_2$ on the structure of high-density lipoprotein and low-density lipoprotein isolated from rapidly salted separated egg yolk. Food Res. Int. 173:113413.

Liu, Y., M. Qing, J. Zang, Y. Chi, and Y. Chi. 2023b. Effects of $CaCl_2$ on salting kinetics, water migration, aggregation behavior and protein structure in rapidly salted separated egg yolks. Food Res. Int. 163:112266.

Liu, Y., X. Yang, Y. Chi, and Y. Chi. 2023c. Effects of $CaCl_2$ on the rheology, microstructure and protein structures of rapidly salted separated egg yolk. Food Res. Int. 172:113096.

Lu, F., Y. Chi, and Y. Chi. 2024. High-temperature glycosylation of saccharides to modify molecular conformation of egg white protein and its effect on the stability of high internal phase emulsions. Food Res. Int. 176:113825.

Lu, F., Y. Ma, J. Zang, M. Qing, Z. Ma, Y. Chi, and Y. Chi. 2023. High-temperature glycosylation modifies the molecular structure of ovalbumin to improve the freeze-thaw stability of its high internal phase emulsion. Int. J. Biol. Macromol. 233:123560.

Ma, Z., Y. Chi, and Y. Chi. 2023. Cryoprotective role of saccharides in frozen egg yolks: water/ice tailoring effect and improved freeze −thaw stability. Food Hydrocoll. 145:109161.

Ma, Z., Y. Chi, H. Zhang, Y. Chi, and Y. Ma. 2022. Inhibiting effect of dry heat on the heat-induced aggregation of egg white protein. Food Chem. 387:132850.

Ma, Z., Y. Ma, R. Wang, and Y. Chi. 2021. Influence of antigelation agents on frozen egg yolk gelation. J. Food Eng. 302:110585.

Nagarajan, M., S. Benjakul, T. Prodpran, P. Songtipya, and H. Kishimura. 2012. Characteristics and functional properties of gelatin from splendid squid (*Loligo formosana*) skin as affected by extraction temperatures. Food Hydrocoll. 29:389–397.

Primacella, M., T. Wang, and N. C. Acevedo. 2018. Use of reconstituted yolk systems to study the gelation mechanism of frozen-thawed hen egg yolk. J. Agric. Food Chem. 66:512–520.

Qing, M., J. Zang, Y. Ma, Y. Chi, and Y. Chi. 2023. Effects of rice vinegar treatment on the antioxidant activities and protein structures of whole egg liquid before and after gastrointestinal digestion. Food Chem. 404:134574.

Rahman, M., K. M. Machado-Velasco, M. E. Sosa-Morales, and J. Vélez-Ruiz. 2009. Freezing point: Measurement, data, and prediction. Pages 153−192 in Food Properties Handbook. M. S. Rahman, ed. CRC Press, Boca Raton.

Rahman, M. S. 2004. State diagram of date flesh using differential scanning calorimetry (DSC). Int. J. Food Prop. 7:407–428.

Rahman, M. S., S. S. Sablani, N. Al-Habsi, S. Al-Maskri, and R. Al-Belushi. 2005. State diagram of freeze-dried garlic powder by differential scanning calorimetry and cooling curve methods. J. Food Sci. 70:E135–E141.

Sahin, S., and S. G. Sumnu. 2006. Rheological properties of foods. Pages 39−105 in Physical Properties of Foods. S. Sahin and S. G. Sumnu, eds. Springer, New York.

Scettri, A., and E. Schievano. 2022. Quantification of polyols in sugar-free foodstuffs by qNMR. Food Chem. 390:133125.

Su, H., J. Tu, M. Zheng, K. Deng, S. Miao, S. Zeng, B. Zheng, and X. Lu. 2020. Effects of oligosaccharides on particle structure, pasting and thermal properties of wheat starch granules under different freezing temperatures. Food Chem. 315:126209.

Sviech, F., J. Ubbink, and A. S. Prata. 2021. Analysis of the effect of sugars and organic acids on the ice melting behavior of pitanga and araza pulp by differential scanning calorimetry (DSC). Thermochim. Acta 700:178934.

Syamaladevi, R. M., S. S. Sablani, J. Tang, J. Powers, and B. G. Swanson. 2009. State diagram and water adsorption isotherm of raspberry (*Rubus idaeus*). J. Food Eng. 91:460–467.

Tan, M., Z. Ding, and J. Xie. 2022. Freezing-induced myofibrillar protein denaturation: contributions of freeze-concentration and role of cellobiose. J. Food Eng. 329:111076.

Tee, E.-T., and L.-F. Siow. 2014. Physical and sensory properties of frozen spanish mackerel (*scomberomorus guttatus*) fish balls added with cryoprotectants. Food Bioproc. Tech. 7:3442–3454.

Tian, J., N. Walayat, Y. Ding, and J. Liu. 2022. The role of trifunctional cryoprotectants in the frozen storage of aquatic foods: recent developments and future recommendations. Compr. Rev. Food Sci. Food Saf. 21:321–339.

Tian, Y., Z. Zhu, and D. Sun. 2020. Naturally sourced biosubstances for regulating freezing points in food researches: fundamentals, current applications and future trends. Trends. Food Sci. Technol. 95:131–140.

Uysal, R. S., and I. H. Boyaci. 2020. Authentication of liquid egg composition using ATR-FTIR and NIR spectroscopy in combination with PCA. J. Sci. Food Agric. 100:855–862.

Van Canneyt, K., and P. Verdonck. 2014. 10.02 - Mechanics of biofluids in living body. Pages 39−53 in Comprehensive Biomedical Physics. A. Brahme, ed. Elsevier, Oxford.

Vivian, J. T., and P. R. Callis. 2001. Mechanisms of Tryptophan fluorescence shifts in proteins. Biophys. J. 80:2093–2109.

Wang, R., Y. Ma, Z. Ma, Q. Du, Y. Zhao, and Y. Chi. 2020. Changes in gelation, aggregation and intermolecular forces in frozen-thawed egg yolks during freezing. Food Hydrocoll. 108:105947.

Wang, R., Y. Ma, L. Zhang, Z. Zhang, Y. Chi, and Y. Chi. 2021a. Changes in egg yolk gelation behaviour and mechanisms during freezing. LWT 151:112223.

Wang, R., L. Zhang, Y. Chi, and Y. Chi. 2022. Forces involved in freeze-induced egg yolk gelation: Effects of various bond dissociation reagents on gel properties and protein structure changes. Food Chem. 371:131190.

Wang, X., J. Li, Y. Su, C. Chang, and Y. Yang. 2021b. Freeze-thaw treatment assists isolation of IgY from chicken egg yolk. Food Chem. 364:130225.

Wang, Z., X. Duan, G. Ren, J. Guo, J. Ji, Y. Xu, W. Cao, L. Li, M. Zhao, Y. Ang, X. Jin, B. Bhandari, L. Zhu, and Y. Zhang. 2023. Improving effect of disaccharides and maltodextrin on preparation of egg yolk powder by microwave-assisted freeze-drying: Functional properties, structural properties, and retention rate of active IgY. Food Chem. 404:134626.

Xu, X., Z. Li, Q. Tang, B. Chen, H. Jin, Y. Yang, D. Shu, Z. Cai, and L. Sheng. 2024. Exploring xylitol as a low-salt alternative for effective inhibition of gelation in frozen egg yolks. Food Chem. 436:137681.

Zang, J., M. Qing, Y. Ma, Y. Chi, and Y. Chi. 2023. Shelf-life modeling for whole egg powder: application of the general stability index and multivariate accelerated shelf-life test. J. Food Eng. 340:111313.

Zhang, B., H. Cao, H. Lin, S. Deng, and H. Wu. 2019. Insights into ice-growth inhibition by trehalose and alginate oligosaccharides in peeled Pacific white shrimp (*Litopenaeus vannamei*) during frozen storage. Food Chem. 278:482–490.

Zhao, A., P. Shi, R. Yang, Z. Gu, D. Jiang, and P. Wang. 2022. Isolation of novel wheat bran antifreeze polysaccharides and the cryoprotective effect on frozen dough quality. Food Hydrocoll. 125:107446.

Zhao, W., Y. Chi, and Y. Chi. 2023a. Saccharides alleviate the thermal instability behavior of liquid egg yolk: influence on rheology property, emulsifying property and protein conformation. Food Hydrocoll. 143:108853.

Zhao, W., Y. Chi, and Y. Chi. 2024. Tracking transformation behavior of soluble to insoluble components in liquid egg yolk under heat treatment and the intervention effect of xylitol. Int. J. Biol. Macromol. 254:127272.

Zhao, W., J. Zang, M. Qing, H. Wang, Y. Chi, and Y. Chi. 2023b. The thermal behavior of egg yolk involves lipoprotein instability. J. Food Eng. 343:111370.

Zheng, H. 2019. Introduction: Measuring rheological properties of foods. Pages 3−30 in Rheology of Semisolid Foods. H. S. Joyner, ed. Springer, Cham.

Zhu, H., J. Li, Y. Su, L. Gu, C. Chang, and Y. Yang. 2023. Sugar alcohols as cryoprotectants of egg yolk: inhibiting crystals and interactions. J. Food Eng. 342:111360.

Zhu, S., J. Yu, X. Chen, Q. Zhang, X. Cai, Y. Ding, X. Zhou, and S. Wang. 2021. Dual cryoprotective strategies for ice-binding and stabilizing of frozen seafood: a review. Trends. Food Sci. Technol. 111:223–232.

Zou, Q., S. M. Habermann-Rottinghaus, and K. P. Murphy. 1998. Urea effects on protein stability: hydrogen bonding and the hydrophobic effect. Proteins. 31:107–115.